Model initial-data problem in stimulated Raman scattering

D. J. Kaup
Clarkson University, Potsdam, New York 13699-5815

C. R. Menyuk
Department of Electrical Engineering, University of Maryland, Baltimore, Maryland 21228

(Received 16 February 1990)

With use of a model set of initial data, the scattering data for stimulated Raman scattering are obtained. For a small Stokes envelope, the scattering data consist only of solitons, each of which is roughly stationary, but with a uniformly growing amplitude. When the Stokes envelope dominates, the scattering data consist of only a continuous spectrum.

I. INTRODUCTION

In a recent article,[1,2] one of the authors (D.J.K.) and Steudel[3] have presented a method of solution for stimulated Raman scattering (SRS). The method of solution for the general SRS equations, including molecular depletion, was presented in Refs. 1 and 3, with the soliton solutions being presented and discussed by Steudel.[3] When the molecular levels are not significantly depleted, the equations in Ref. 1 reduce to the normalized set

$$\partial_\chi A_1 = -XA_2 \ , \tag{1a}$$

$$\partial_\chi A_2 = X^* A_1 \ , \tag{1b}$$

$$\partial_\tau X + \gamma X = A_1 A_2^* \ , \tag{1c}$$

where χ and τ are the co-moving coordinates

$$\chi = z \ , \tag{2a}$$

$$\tau = t - z/u \ , \tag{2b}$$

with z being the propagation direction, t the time, and u the common group velocity of A_1 and A_2 in the medium. The quantity X describes the material excitation. The quantity A_1 is the envelope of the pump wave, while A_2 is the envelope of the Stokes wave. The quantity γ gives the damping rate of the material excitation due to collisions. Equations (1) were shown to be integrable by Chu and Scott[4] when $\gamma = 0$. However, the initial value problem that they solved was not the one of physical interest. The physically interesting initial-value problem is where one is given $A_1(\chi=0)$, $A_2(\chi=0)$, and $X(\tau=0)$. It was recently solved by Kaup[2] using an infinite-interval inverse scattering transform (IST) to solve a finite-interval problem. And most unusually, he found that this solution could have solitons with time-dependent eigenvalues.[1] (This was very remarkable for an integrable system.) As is well known, all solitons (at least on an infinite interval) have eigenvalues which are constant in time. So what is happening in this finite-interval integrable system?

At this point, we should make some remarks concerning SRS solitons[5,6] and how they differ from other solitons. The soliton solution of (1) is

$$A_1 = \frac{A(\tau)e^{i\phi}}{\cosh Z} \ , \tag{3a}$$

$$A_2 = A(\tau)\tanh Z \ , \tag{3b}$$

$$X = \frac{2\eta e^{i\phi}}{\cosh Z} \ , \tag{3c}$$

where $A(\tau)$ is arbitrary and real, η and ϕ are real constants, and

$$Z = 2\eta\chi - \frac{1}{2\eta}\int_0^\tau A^2(\tau)d\tau \ . \tag{4}$$

In the above, η is also the soliton's eigenvalue. This soliton exists on the background of the Stokes envelope. For Z large, the pump wave is zero while the Stokes wave is not. Thus it cannot develop until the pump wave (A_1) has been mode converted into the Stokes wave (A_2). After this occurs, then the SRS soliton given by (3) could be expected to be observed. It represents a phase flip on the Stokes envelope, with a (transient) reversal of the pump depletion in the region of the phase flip. From (2) and (4), the SRS soliton moves with velocity

$$\frac{dx}{dt} = u\frac{A^2}{A^2 + \eta^2 u} \ , \tag{5}$$

which is less than the group velocity u. Thus for any finite energy in the pump pulse, the SRS soliton then will always slip toward the back of the pump envelope, eventually falling off onto the tail where A^2 becomes vanishing small. The SRS soliton effectively dies and vanishes. Because of this, SRS solitons are called transient solitons.[6]

In most integrable systems, solvable by IST, initial data will break up into a number of solitons and a continuum. By contrast, numerical studies of Eq. (1) in the limit where γ can be neglected show quite different behavior.[7,8] There are three distinct evolution regimes. In the first regime, the I regime, the Stokes wave is small compared to the pump wave and grows exponentially. In the next regime, the transition regime, the Stokes and pump waves have roughly equal amplitudes. In the final regime, the J regime, the integrated pump intensity de-

creases algebraically as $\chi^{-1/4}$, while the pump amplitude develops oscillations whose frequency increases as $\chi^{1/4}$. Indeed, Menyuk[6] proved that at least the material excitation must always tend toward zero. This behavior is not solitonlike, but must be consistent with the solution obtained by IST. The J-regime behavior is shown in Figs. 1 and 2 when the Stokes intensity is initially proportional to the pump intensity.

To compare the results of IST to the known behavior of the solution, we consider the simple model

$$A_1(\chi=0)=a(\tau)\cos\Delta\ , \tag{6a}$$

$$A_2(\chi=0)=a(\tau)\sin\Delta\ , \tag{6b}$$

$$X(\tau=0)=0\ , \tag{6c}$$

where a is real and Δ is some constant. This case experimentally corresponds to the creation of a pump and a Stokes envelope whose ratio is constant; a situation which could be approximately obtained in the laboratory. It also corresponds to having all scattering data for the IST vanish at $\tau=0$. Thus it would seem to be a trivial case at first. But most surprising, the χ evolution of the initially trivial scattering data blooms instantly into a countable infinity of solitons, each one of which has an eigenvalue which increases in time. And one can obtain a closed-form solution for the scattering coefficients as well as for all the soliton parameters. Furthermore, the scattering data consist of only a countable infinity of solitons. There is no continuous spectrum (also called radiation). The solution is an exact N-soliton solution where N is taken to be infinity.

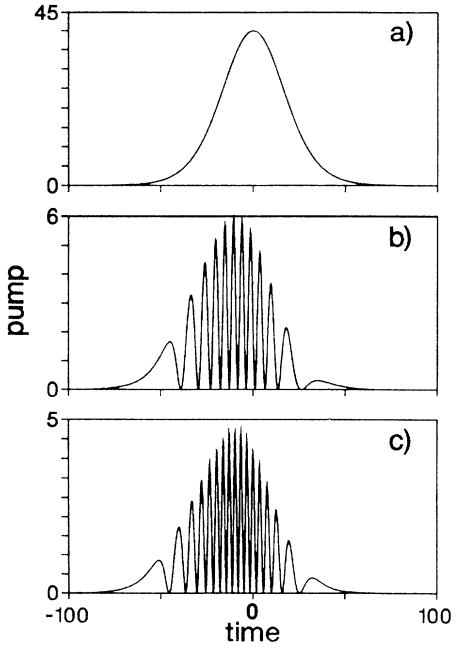

FIG. 1. The pump intensity as a function of time at increasing distances in physical units. Pump intensity is measured in GW/cm^2 and time is measured in picoseconds. The distances are sufficiently large that the pump oscillations due to narrowing of the soliton widths are clearly apparent. (This figure is the same as Fig. 10 of Ref. 8.)

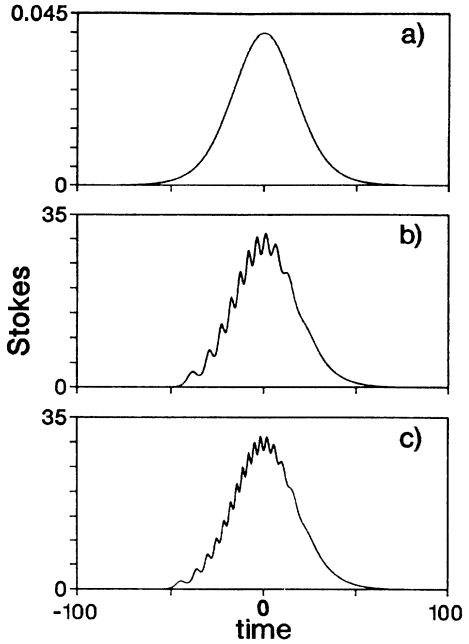

FIG. 2. The Stokes intensity at the same distances as in Fig. 1. The physical units are also as in Fig. 1. Note that the Stokes intensity takes on the original shape of the pump intensity but at a lower intensity. While the number of Stokes photons ultimately equals the number of pump photons, the energy per photon of the Stokes wave is lower, leading to a lower intensity. The energy difference goes into the material excitation. (This is the same as Fig. 11 of Ref. 8.)

Since all the eigenvalues increase with time, these solitons cannot be transient. So how could one reconcile this soliton behavior with the physics of SRS described earlier? We shall find that all of these solitons are located near $T=0$ and that their widths decrease as χ increases. The accumulation of all these solitons near the origin of the physical time domain must lead to the observed oscillatory behavior of the pump, but a detailed proof remains to be accomplished.

In Sec. II, we shall briefly review the method of solution for SRS proposed by Kaup. Then in Sec. III we shall analyze the scattering data for the Menyuk case, Eq. (6).

II. THE SOLUTION OF SRS BY THE METHOD OF THE IST

According to Kaup (Ref. 2, Sec. 2), from the initial data, one constructs the functions

$$S_3=\tfrac{1}{4}(A_1^*A_1-A_2^*A_2)\ , \tag{7a}$$

$$S_+=\frac{i}{2}A_2^*A_1\ , \tag{7b}$$

$$S_-=S_+^* \tag{7c}$$

at $\chi=0$. One defines

$$A(\tau)=\tfrac{1}{4}(A_1^*A_1+A_2^*A_2)\ , \tag{8}$$

which is the total intensity, and the angles β and θ by

$$S_3 = A\cos\beta \ , \tag{9a}$$

$$S_+ = Ae^{i\theta}\sin\beta \ . \tag{9b}$$

One next constructs the functions T and q:

$$T = \int_{-\infty}^{\tau} A(\tau)d\tau \ , \tag{10}$$

$$q = \frac{i}{2\cos\beta}\partial_T(e^{i\gamma}\sin\beta) \ , \tag{11}$$

where

$$\gamma(T) = \int_0^T (\cos\beta)(\partial_T\theta)dT \ . \tag{12}$$

The quantity T is called the "nonlinear time," and q is the potential in the well-known Zakharov-Shabat (ZS) eigenvalue problem[9]

$$\partial_T v_1 + i\zeta v_1 = qv_2 \ , \tag{13a}$$

$$\partial_T v_2 - i\zeta_2 = -q^* v_1 \ , \tag{13b}$$

where ζ is the spectral parameter. Note that for a finite-energy pulse, the integral in (10) is bounded by

$$0 < T < T_\infty = \int_{-\infty}^{\infty} A(\tau)d\tau < \infty \ . \tag{14}$$

Thus the ZS eigenvalue problem is on a finite interval. Note that it is the nonlinear time T that is on a finite interval and not the linear time τ, which is on the infinite interval, $-\infty < \tau < \infty$.

Given q at $\chi = 0$, one solves (13) on the finite interval, $0 \le T \le T_\infty$. The Jost function $\phi(T,\chi)$ satisfies (13) and the boundary condition

$$\phi(T=0,\chi=0) = \begin{bmatrix} 1 \\ 0 \end{bmatrix} \ . \tag{15}$$

At the other end of the finite interval,

$$\phi(T_\infty,\chi=0) = \begin{bmatrix} ae^{i\zeta T_\infty} \\ be^{-i\zeta T_\infty} \end{bmatrix} \ , \tag{16}$$

where a and b are called the scattering coefficients. The conjugate set of scattering coefficients is

$$\bar{a}(\zeta) = a^*(\zeta^*) \ , \tag{17a}$$

$$\bar{b}(\zeta) = b^*(\zeta^*) \ , \tag{17b}$$

and these scattering coefficients satisfy

$$\bar{a}a + \bar{b}b = 1 \tag{18}$$

on the real-ζ axis.

Given these scattering coefficients, one may reconstruct the potential q, the Jost function ϕ, and also the angles β and θ.[1] To do this, one first needs to construct the function

$$G(z) = \frac{1}{2\pi}\int_C \frac{\bar{b}}{a}e^{-i\zeta z}d\zeta \tag{19}$$

in the finite interval $0 < z < 2T_\infty$, where the contour C is the standard complex-ζ contour, which goes over and above all zeros of $a(\zeta)$ in the upper-half complex-ζ plane. Then one solves the linear integral equations,[10]

$$\bar{L}(x,y) + \begin{bmatrix} 1 \\ 0 \end{bmatrix} G(x+y) - \int_0^x L(x,s)G(s+y)ds = 0 \ , \tag{20a}$$

$$L(x,y) + \begin{bmatrix} 0 \\ 1 \end{bmatrix} \bar{G}(x+y) + \int_0^x \bar{L}(x,s)\bar{G}(s+y)ds = 0 \ , \tag{20b}$$

for the column matrices $L(x,y)$ and $\bar{L}(x,y)$ for $x > y$. The potential is recovered from

$$q(T) = 2\bar{L}_1(T,T) \ , \tag{21}$$

and the Jost function (15) is

$$\phi = \begin{bmatrix} 1 \\ 0 \end{bmatrix} e^{-i\zeta T} - \int_0^T L(T,s)e^{-i\zeta s}ds \ . \tag{22}$$

Thus if we know how $\bar{b}$ and a evolve in χ, we can evaluate $G(z)$ at any χ and thereby be able to construct the solution for A_1 and A_2 at any χ. The χ evolution of a and $\bar{b}$ is[1-3]

$$\partial_\chi a = \frac{i}{\zeta}(\cos\beta_\infty - \cos\beta_0)a - \frac{\sin\beta_0}{\zeta}\bar{b} + \frac{\sin\beta_\infty}{\zeta}be^{2i\zeta T_\infty} \ , \tag{23a}$$

$$\partial_\chi \bar{b} = \frac{i}{\zeta}(\cos\beta_\infty + \cos\beta_0)\bar{b} + \frac{\sin\beta_0}{\zeta}a - \frac{\sin\beta_\infty}{\zeta}\bar{a}e^{-2i\zeta T_\infty} \ , \tag{23b}$$

where

$$\beta_0 = \beta(T=0) \ , \tag{24a}$$

$$\beta_\infty = \beta(T=T_\infty) \ , \tag{24b}$$

and with similar equations for $\bar{a}$ and b. The difficulty with the above χ evolution is that one must know $\beta_\infty(\chi)$ before one can solve (23) for $a(\chi)$ and $\bar{b}(\chi)$. While one can control $\beta_0(\chi)$ experimentally, one has no control over $\beta_\infty(\chi)$. In fact, its value is determined by the evolution of the SRS equation and is *not* an independent set of data. However, as noted by Kaup,[1] since we are working with a finite-interval problem, one may actually ignore these terms in (23), because these terms will only affect the values of $G(z)$ for $z \ge 2T_\infty$. Since this is outside the range of physical interest, we may set

$$\beta_\infty = 0 \tag{25}$$

in (25) and still obtain correct values for $G(z)$ in the interval $0 \le z < 2T_\infty$. Thus the χ-evolution equations to be solved are

$$\partial_\chi a = \frac{i}{\zeta}(1-\cos\beta_0)a - \frac{\sin\beta_0}{\zeta}\bar{b} \ , \tag{26a}$$

$$\partial_\chi \bar{b} = \frac{i}{\zeta}(1+\cos\beta_0)\bar{b} + \frac{\sin\beta_0}{\zeta}a \ . \tag{26b}$$

Note that if $X(\tau\to-\infty)\to 0$, then by (1), (9), and (11), we have

$$\partial_\chi \beta_0 = 0 \ . \tag{27}$$

Otherwise, if $X(\chi,\tau\to-\infty)$ were nonzero, one would simply integrate with respect to χ for $\tau\to-\infty$ to determine $\beta_0(\chi)$.

We also wish to mention that (26) arises also in superfluorescence, and the identical equations have also been given by Steudel.[11] Next we shall look at the Menyuk initial-value problem as given by (6), obtaining the solutions for a, $\bar{b}$, and G.

III. RESOLUTION OF THE INITIAL-VALUE DATA INTO SCATTERING DATA

First, we evaluate A, β, θ, and γ at $\chi=0$ from Eqs. (6)–(9). One obtains

$$A(\tau)=\tfrac{1}{4}a[(\tau)]^2 \ , \tag{28a}$$

$$\theta(\chi=0)=\theta_0=\pi/2 \ , \tag{28b}$$

$$\beta(\chi=0)=\beta_0=2\Delta \ , \tag{28c}$$

then by (11) and (12),

$$\gamma(\chi=0)=\gamma_0=0 \ , \tag{28d}$$

$$q(\chi=0)=0 \ , \tag{29}$$

since it is given under (6) that

$$\partial_T \Delta = 0 \ . \tag{30}$$

As a consequence of (24), it follows that, at $\chi=0$, (13) only has the trivial solution for the Jost function. Upon writing it out, from (16) we have the trivial scattering data

$$a(\chi=0)=1 \ , \tag{31a}$$

$$\bar{b}(\chi=0)=0 \ . \tag{31b}$$

We now evolve these scattering coefficients in χ via (28). The result is

$$a(\chi)=\tfrac{1}{2}(1-\cos\beta_0)e^{2i\chi/\zeta}+\tfrac{1}{2}(1+\cos\beta_0) \ , \tag{32a}$$

$$\bar{b}(\chi)=-\frac{i}{2}(e^{2i\chi/\zeta}-1)\sin\beta_0 \ . \tag{32b}$$

The bound-state spectrum is determined by the zeros of a in the upper-half ζ plane. These occur at

$$\zeta_n=\frac{\chi}{\pi(n+\frac{1}{2})-i\kappa} \ , \tag{33}$$

where n is any integer and

$$\kappa=\tfrac{1}{2}\ln\left[\frac{1+\cos\beta_0}{1-\cos\beta_0}\right] \ . \tag{34}$$

For $0<\beta_0<\pi/2$, we have $\kappa>0$, and all zeros of $a(\chi)$ lie in the upper half ζ plane. Each of these zeros is a bound state for (13), and each bound state corresponds to a soliton. Thus we have a countable infinity of solitons. If $\pi/2<\beta<\pi$ (where the Stokes pulse dominates), then $\kappa<0$ and all zeros lie in the lower half ζ plane. Now there are no bound states and no solitons.

In addition to the bound-state eigenvalue, the scattering data require a normalization coefficient at each eigenvalue.[10] These are

$$D_n\equiv\frac{b(\zeta_n)}{\partial_\zeta a(\zeta_n)} \tag{35}$$

$$=\frac{\zeta_n^2}{\chi\sin\beta_0} \ . \tag{36}$$

Note that even if $\kappa<0$ (33) is still the zeros of $a(\zeta)$ and (36) is still valid. We shall return to this point shortly.

In addition to the bound-state spectrum, there is also the continuous spectrum, or radiation. However, as we shall now show, the continuous spectrum for $\kappa>0$ is absent, while for $\kappa<0$, the continuous spectrum, is equivalent to an infinite set of "virtual solitons."

Now let us evaluate $G(z)$. First, observe that in the upper half ζ plane, as $|\zeta|\to\infty$, a and $\bar{b}$ both become independent of ζ. Thus for $z<0$ the contour in (19) may be pushed out to infinity, giving

$$G(z)=0 \quad \text{if } z<0 \ . \tag{37}$$

For $z>0$, one could close the contour in (19) from below. Then the value of $G(z)$ would be given as a sum over all the residues at the zeros of a, plus the contribution from the essential singularity (cluster point) at $\zeta=0$. This latter can be shown to be zero as follows. From (32) one has

$$\frac{\bar{b}}{a}=\frac{-i\sin\beta_0(e^{2i\chi/\zeta}-1)}{e^{2i\chi/\zeta}(1-\cos\beta_0)+(1+\cos\beta_0)} \ . \tag{38}$$

As $|\zeta|\to 0$ in the upper half ζ plane and for $\chi>0$,

$$\frac{\bar{b}}{a}\to -i\frac{\sin\beta_0}{1-\cos\beta_0} \ , \tag{39a}$$

while for $|\zeta|\to 0$ in the lower half ζ plane and $\chi>0$,

$$\frac{\bar{b}}{a}\to\frac{i\sin\beta_0}{1+\cos\beta_0} \ . \tag{39b}$$

From (39) it is clear that as $|\zeta|\to 0$, $\bar{b}/a$ can only be singular along the real axis. Therefore if we can construct an arbitrary small contour encircling the origin, which crosses the real axis where $\bar{b}/a$ can be bounded uniformly, then the contribution of the cluster point to $G(z)$ will vanish. A series of such contours is given by

$$\left\{C_n:\zeta=\frac{\chi}{\pi n e^{i\theta}-i\kappa}\right\} \ , \tag{40}$$

where n is any integer and θ is the real parameter which rolls out the contours. These contours pass through the valley between two adjacent poles of $\bar{b}/a$. Along the nth contour,

$$\bar{b}/a|_{C_n}=\frac{-i\cos\beta_0}{\sin\beta_0}+\frac{\sin(2\pi n\cos\theta)+i\sinh(2\pi n\sin\theta)}{2\sin\beta_0[\sinh^2(\pi n\sin\theta)+\cos^2(n\pi\cos\theta)]}\ . \tag{41}$$

It is now rather elementary to show that for all θ

$$|\bar{b}/a|_{C_n}|^2<(5/\sin\beta_0)^2<\infty\ . \tag{42}$$

Thus we have

$$\lim_{n\to\infty}\left|\int_{C_n}d\zeta(\bar{b}/a)e^{i\zeta z}\right|\to 0\ , \tag{43}$$

and therefore

$$G(z)=-i\sum_{n=-\infty}^{\infty}D_n e^{-i\zeta_n z} \tag{44}$$

for $z>0$. What (44) shows is that for $\kappa>0$, only the bound states or solitons contribute to $G(z)$. There is no radiation or continuous spectrum. That vanished because there was no contribution from the cluster point.

Now, for $\kappa<0$, it turns out that (44) is valid for $G(z)$, although all the zeros of a are in the lower half ζ plane. In this case $G(z)$ can first be reduced from (19) to an integral along the real ζ axis. This integral, in the infinite-interval case, is over a continuous spectrum of ζ with $b/a(\zeta)$ giving the amplitude of each spectrum component. However, this continuous integral can be evaluated as described above, by closing the contour in the lower half ζ plane. And the contributions from all the residues are as in (44), except that now the imaginary parts of ζ_n are in the lower half plane instead of the upper half. So for $\kappa<0$, only the radiation contributes to $G(z)$. However, this contribution can be given in terms of a countable infinity of virtual solitons, each of which has an eigenvalue in the lower half plane.

IV. CONCLUSION AND INTERPRETATION OF THE SOLUTION

At the moment, it does not seem to be possible to construct the N-soliton solution required for this problem. But there are some interesting features of the solution which should be noted. First, let us construct a one-soliton solution from

$$G(z)=iD_1e^{-i\zeta_1 z}\ . \tag{45}$$

Then from (19) and (21) we have

$$q(T)=\frac{2iD_1e^{-2i\zeta_1 T}}{1+|D_1/2\eta_1|^2(e^{2\eta_1 T}-1)^2}\ , \tag{46}$$

where η_1 is the imaginary part of ζ_1. This soliton shape differs from the usual ZS soliton because the integrals in (20) start at zero and not minus infinity. This is the first different feature.

If we ask where the maximum of this soliton is, from (46) one readily obtains

$$4\eta_1T_0=\ln(1+|2\eta_1/D_1|^2)\ , \tag{47}$$

where T_0 is the location of the soliton's maximum. From (33) and (36),

$$\eta_n=\frac{\chi\kappa}{(n+\frac{1}{2})^2\pi^2+\kappa^2}\ , \tag{48}$$

$$\left|\frac{D_n}{2\eta_n}\right|=\left|\frac{1}{2\kappa\sin\beta_0}\right|\ , \tag{49}$$

where the latter is independent of the index n. As a consequence of (47) and (49), we have

$$4\eta_1T_0=\ln(1+4\kappa^2\sin^2\beta_0)\ . \tag{50}$$

In the usual experimental situation, one would have a smaller Stokes pulse with β_0 very small. The η_1T_0 would be also very small. The implication of this is the worst possible situation for an N-soliton configuration. Namely, all solitons are only a small fraction of their own soliton width from the origin ($T=0$), with the center of each soliton located just slightly into the physical region ($T>0$). In simple terms, all the solitons are piled on top of each other somewhere near $T=0$. The simple one-soliton formula (48) indicates that they are centered near $T=0$. But one should be careful using this formula, because in general there are phase shifts when solitons pass through one another. However, here the solitons cannot be easily identified and separated because no one soliton appears to be in front of the rest. Thus we should be careful in assigning any location to any one of these solitons. The best that we can say is that they are roughly all within their own soliton's width of each other.

But the one thing that does change is their width. They uniformly become narrower as the cell length χ is increased. For small χ, all eigenvalues are small and all solitons are very broad. Since the physical region is from $0<T<T_\infty$, there is a range of χ around $\chi=0$ where all soliton widths are greater than T_∞ (i.e., $\eta_nT_\infty\ll 1$). Here the solution for q is more or less constant in T but increasing in χ. As χ becomes larger, such that $\eta_1T_\infty\simeq 1$, then the first soliton is almost entirely inside the physical region, and the solution starts to demonstrate variations in T. As χ becomes even larger, more and more solitons "become active" in the physical region of $0<T<T_\infty$. Thus this solution is consistent with the observed numerical results.[7,8] In fact, one can see in Fig. 2 the general decrease in the oscillation widths and the general movement of the oscillations to the rear of the pulse.

From (48) we can estimate the number of active solitons N at any cell length to be

$$N\simeq\frac{2}{\pi}\chi\kappa T_\infty\ ; \tag{51}$$

the factor of 2 comes from the fact that negative integers are also allowed. For values of $|n|>N$, the solitons are too broad to be sensed.

In conclusion, we have found the Menyuk initial data to represent a very interesting style of soliton evolution. The solitons remain almost stationary, but their amplitude grows uniformly. In other soliton systems, the opposite occurs.

Note added in proof. Although the main purpose of our paper was to study a model initial-value problem for SRS and to investigate the χ evolution of the scattering data, it has been recently pointed out by Steudel[11] that this solution can also be obtained from the similarity solution of the sine-Gordon equation. When the damping is zero and θ is constant, then (1) can be reduced to[12]

$$\partial_\chi \partial_T \beta = 4 \sin\beta \ . \tag{52}$$

A similarity solution of this equation is $\beta(\chi,T)=f(4\chi T)$, where $f(z)$ satisfies[13]

$$zf''+f'=\sin f \ . \tag{53}$$

To obtain the solution for (6), one simply takes the regular solution of (53) for the initial value of $f(0)=2\Delta$.

Equation (53) is a special case of the third Painlevé equation (PIII) (third Painlevé transcendent) whose solution for the case $f=iu$ has been given by Flaschka and Newell[14] by a singular integral equation. The general solution for PIII has been given by Fokas, Mugan, and Ablowitz[15] as a transformation on PV, where the solution of PV is also given by singular integral equations. On the other hand, we have a solution of (53) which is given by the well-known Gelfand-Levitan-Marchenko integral equation (20). Our thanks to Dr. Steudel for pointing out that our solution can be given by the similarity solution of (53).

ACKNOWLEDGMENTS

This work has been supported in part by the National Science Foundation through Grant No. DMS-8803471, and by the U.S. Air Force of Scientific Research through Grant No. AFOSR-86-0277. Dr. Menyuk's research was supported by the Naval Research Laboratory, and the numerical simulations reported in Figs. 1 and 2 were carried out at the San Diego Super Computing Center.

[1]D. J. Kaup, Physica **6D**, 143–54 (1983).
[2]D. J. Kaup, Physica **19D**, 125–134 (1986).
[3]H. Steudel, Physica **6D**, 155 (1983).
[4]F. Y. F. Chu and A. C. Scott, Phys. Rev. A **12**, 2060 (1975).
[5]K. Druhl, R. G. Wenzel, and J. L. Carlsten, Phys. Rev. Lett. **51**, 1171 (1983).
[6]Curtis R. Menyuk, Phys. Rev. Lett. **62**, 2937 (1989).
[7]C. R. Menyuk and G. Hilfer, Opt. Lett. **14**, 227 (1989).
[8]G. Hilfer and C. R. Menyuk, J. Opt. Soc. Am. B **7**, 739 (1990).
[9]V. E. Zakharov and A. B. Shabat, Zh. Eksp. Teor. Fiz. **61**, 118 (1971) [Sov. Phys.—JETP **34**, 62 (1972)].
[10]M. J. Ablowitz, D. J. Kaup, A. C. Newell, and H. Segur, Stud. Appl. Math. **53**, 249 (1974).
[11]H. Steudel (private communication).
[12]H. Steudel, Ann. Phys. **34**, 188 (1977).
[13]G. L. Lamb, Jr., Phys. Lett. **29A**, 507 (1969).
[14]Hermann Flaschka and Alan C. Newell, Math. Phys. **76**, 65 (1980).
[15]A. S. Fokas, U. Mugan, and M. J. Ablowitz, Physica D **30**, 247 (1988).